Journal of Engineering Science and Technology
Vol. 21, No. 3 (2026) 795 - 811

SIMULATION-BASED EVALUATION OF SUN TRACKING SYSTEM FOR ENHANCED SOLAR ENERGY HARVESTING IN MALAYSIA USING MATLAB

SITI NUR AFIFAH MOHD SUHAIMI[1], NOR AIRA ZAMBRI[1,*], FARAHIYAH MUSTAFA[1], NORHAFIZ BIN SALIM[2], MOHAMAD AIMAN ARIF ABU BAKAR[3]

[1]Department of Electrical Engineering Technology, Faculty of Engineering Technology, Universiti Tun Hussein Onn Malaysia, 84600 Pagoh, Johor, Malaysia
[2]Department of Electrical Engineering, Faculty of Electrical Technology and Engineering, Universiti Teknikal Malaysia Melaka, Hang Tuah Jaya, 76100 Durian Tunggal, Melaka, Malaysia
[3]Department of Operation and Maintenance, Solarvest Energy Sdn Bhd (Johor), Jalan Molek 1/5B, Taman Molek, 81100 Johor Bahru, Malaysia
*Corresponding Author: aira@uthm.edu.my

Abstract

Fixed solar panels often suffer from reduced energy capture due to their static orientation, which prevents effective tracking of the sun's movement throughout the day. Although dual-axis solar tracking systems have demonstrated potential worldwide, few studies have examined their application and validation under Malaysia's specific solar conditions. This study proposes a dual-axis solar tracking system designed to improve panel positioning through continuous calculation of the sun's position. The system dynamically adjusts orientation based on local solar time (LST), altitude, azimuth, and tilt angles to maximize energy absorption. Simulations using MATLAB/Simulink were conducted to evaluate performance across different times and dates throughout the year in Malaysia. The model was verified using few sample dates and compared against two web-based solar data tools to confirm accuracy. Solar position data was collected with 15-minute intervals guided panel movement to maintain perpendicular alignment with sunlight. Validation against established solar data tools successfully showed minimal deviation. The proposed results demonstrated significant improvements in maximum power output (P_{max}), voltage (V_{mp}), and current (I_{mp}) which undisputedly highlights the effectiveness of solar tracking in enhancing photovoltaic efficiency and supports Malaysia's renewable energy goals.

Keywords: Altitude angle, Azimuth angle, Dual-axis, LST, MATLAB/Simulink, Solar tracking system, Sun position.

1. Introduction

The rapid growth of solar technology has led to a surge in users installing solar systems, whether on rooftops or in solar power plants, with the intention of replacing coal and gas power generation. However, despite the abundant availability of renewable resources such as solar, tidal, and wind energy, harnessing these resources presents several challenges [1]. Among renewable energy sources, solar energy is the cleanest source, which aligns with the World Sustainable Development Goal 7 [2]. Malaysia is actively working to increase the share of renewable energy in its power capacity mix to 31% by 2025 and 40% by 2035 [3]. The introduction of the feed-in tariff in 2011, along with renewable energy laws, has significantly accelerated the growth of the solar photovoltaic industry in Malaysia until now [4].

According to the Sustainable Energy Development Authority (SEDA), the implementation of the new Net Energy Metering (NEM) regulation has further encouraged solar panel installations as a long-term investment through 2024 [5]. Furthermore, solar irradiance plays a critical role in PV power generation efficiency and is most effective in regions with abundant sunlight, which corresponds well with Malaysia's climate. The amount of irradiance striking the solar cells directly affects a photovoltaic module's power output [6]. Since the sun continuously shifts position in the sky throughout the day from rising in the east to setting in the west [7], understanding the fundamentals of Earth-Sun interaction is essential. The sun's apparent motion and surface geography influence the availability of solar energy. Therefore, a tracking system is necessary to enhance energy production and achieve maximum efficiency in solar photovoltaic systems [8].

The main factors typically considered in modelling solar irradiance on an inclined surface include declination (δ), latitude (φ), surface azimuth angle (σ), angle of incidence (Θ), day of the year (n), hour angle (ω). There is a direct relationship between solar energy generation and solar irradiance. Early solar tracking systems primarily focused on single-axis trackers, which rotate solar panels along one axis typically aligned with the Earth's polar axis [8]. This configuration enables panels to follow the sun's east to west movement across the sky, maintaining a perpendicular orientation to sunlight throughout the day. Single-axis trackers are simpler in design and more cost-effective than dual-axis systems, making them a preferred option for solar farms and installations where budget constraints are a key consideration. Studies, including one by Mohamed Taha et al. [7] have shown that single-axis tracking systems can improve energy capture by approximately 2.6% compared to fixed solar panels. However, despite these advantages, single- axis trackers are unable to adjust for variations in the sun's altitude.

Solar altitude changes throughout the day, rising and falling with the sun's movement across the sky and varying across seasons, making single-axis systems less effective in optimizing energy capture than advanced tracking techniques [9]. The normal vector of the tracked panel is analysed and validated using a solar radiation model along with the geometric relationships between the sun and Earth. Limitations in existing single-axis trackers have been identified, resulting in reduced performance, with only 96.40% of available solar radiation being captured [10]. This constraint reduces the efficiency of single-axis trackers, especially in

regions with significant seasonal shifts in solar altitude, where panels may not maintain at the optimal angle to capture maximum sunlight exposure.

The innovation continues with the dual-axis tracker, which addresses the limitations of single-axis systems by introducing a second axis of rotation. This enhancement enables solar panels to follow the sun's movement both horizontally from east to west and vertically from north to south [11]. Dual-axis trackers allow panels to remain directly aligned with the sun throughout the day, thereby maximizing energy capture as the solar declination angle fluctuates between -23.45° and 23.45° over the course of the year [12]. Compared to fixed systems, dual-axis trackers can increase energy output by up to 3.3% [7], and in certain cases, such as reported by Sharma et al. by as much as 15.69% [13]. These systems typically employ light-dependent resistors (LDRs) to detect sunlight direction and adjust panel angles in real time [14, 15]. Some designs incorporate date and time-based tracking mechanisms with reduction gear units, achieving high accuracy with tracking errors below 0.2°, while offering benefits such as low maintenance and stable movement.

Sowaruth et al. highlight the effectiveness of tilt and azimuth adjustments, particularly under low solar elevation conditions [14]. To overcome sensor limitations, Aristoya et al. developed a fuzzy logic-based dual-axis tracker. In this system, the north south axis adjusts daily based on declination and geographic location, while the east west axis updates every 10 minutes using LDR input and angle comparison [16]. Control and communication are managed via Arduino Mega and ESP-12E microcontrollers. However, trackers that rely on LDRs often lose accuracy in cloudy or rainy conditions, as diffused or obstructed sunlight can impair sensor performance.

Sensor-based solar tracking systems are adaptive but often lose precision in cloudy conditions and require recalibration. Fixed-tilt systems with incident angle optimization are simpler and cost-effective yet limited in efficiency due to their static orientation. To address tracking accuracy, sensor less open-loop systems have gained interest. Jazayeri et al. [17] and Jha and Roy [18] developed MATLAB/Simulink models to calculate solar incidence, azimuth, and altitude angles, offering theoretical improvements in panel orientation. However, their approaches remain unvalidated in real-world conditions and do not provide methods for determining optimal tilt angles across different times and dates, limiting practical application.

Building on these works, the present study introduces a dynamic, validated dual-axis tracking model designed to Malaysia's solar conditions. By integrating local solar time (LST), altitude, and azimuth angles, the model calculates optimal tilt angles and ensures panels remain perpendicular to sunlight throughout the year. Unlike prior studies focused solely on simulations, this work incorporates multi-source validation against established solar data tools, achieving deviations below 1° and demonstrating both accuracy and robustness. The study therefore advances the field by providing a localized, simulation-based framework with practical relevance for tropical climates, guided by two key research questions which are evaluating the accuracy of the proposed model against solar data tools, and assessing the impact of tilt angle adjustment on photovoltaic performance across different times and dates.

2. Methods

The methodology of this study was structured in three main stages. First, a dual-axis solar tracking model was developed using MATLAB/Simulink to calculate solar position parameters. The simulated results were then compared with data obtained from established web-based solar tools to verify the accuracy and reliability of the MATLAB model. Following this validation, the verified model guided the collection of real experimental data, where both tracking and non-tracking solar panel configurations were tested to evaluate differences in energy capture.

2.1. Sun path modelling theory

The sun's trajectory varies throughout the year, influencing daylight duration across different regions and seasons. This paper presents a MATLAB/Simulink model that able to generates a full year of solar position data for a dual-axis photovoltaic (PV) tracking system. The model inputs include local time, longitude, Greenwich Mean Time (GMT), Julian day number, and latitude, while the outputs comprise the solar altitude angle, azimuth angle, local solar time (LST), and panel tilt angle, as shown in Fig. 1. Equations (1)-(12) were used to develop the complete model, and data were collected for one year. The outputs which are altitude angle, azimuth angle, tilt angle, and LST were uploaded to a MAT file in MATLAB and subsequently stored in an Excel sheet. This process ensured that solar tracking data were systematically collected and recorded for further analysis.

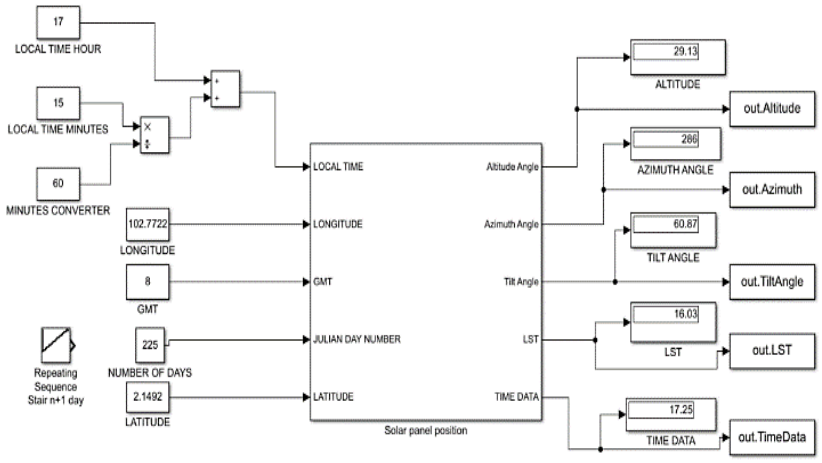

Fig. 1. Simulation model of sun trajectory and solar panel positioning in MATLAB/Simulink.

As illustrated in the flowchart in Fig. 2, the model calculates the sun's azimuth and altitude angles and determines the optimal tilt angle to maintain perpendicular alignment with the sun's rays throughout the day and year. Incorporating tilt angle estimation enhances hardware design accuracy by enabling real-time solar tracking, which represents the key novelty of this study. The model was applied to an eastern subsystem with Malaysia, specifically Muar, Johor, as the study location. Solar movement was simulated using these mathematical models, with LST processed at each instant or interval to obtain the corresponding local solar time.

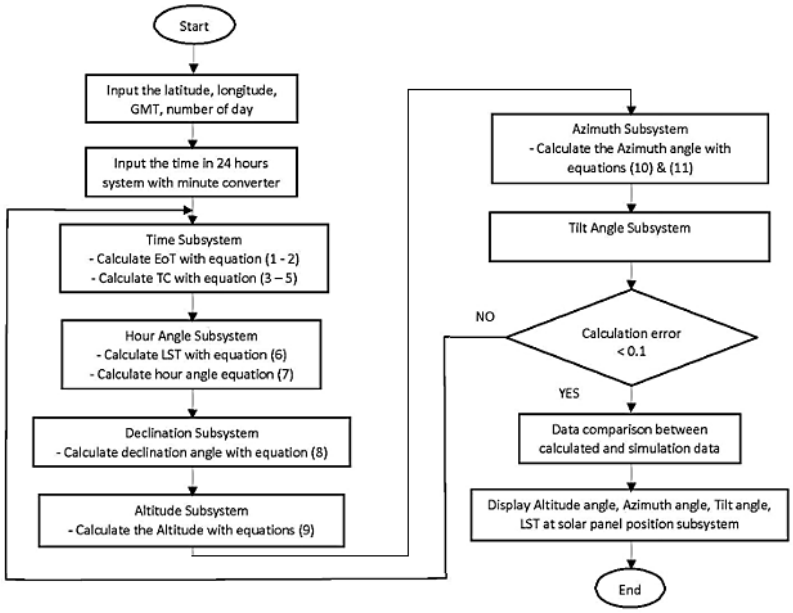

Fig. 2. Flowchart of solar tracking system calculations.

2.2. Local solar time (LST)

The Local Solar Time (LST) represents the actual time based on the sun's position in the sky and differs from standard time due to factors such as longitude and the Equation of Time (EoT). LST is essential for accurately tracking the sun's movement, which governs the orientation of the solar panel. The Time Correction (TC) adjusts the standard local time (LT) which is the official clock time in a region to align with solar time. While longitude determines LT, the sun's apparent motion is independent of geographical time zones and is governed solely by solar time. Consequently, solar noon, corresponding to the sun's highest elevation, may not coincide with 12:00 PM local clock time at a given location. In this simulation, the local clock time of any specified location was converted to LST, which was then used to determine the sun's position and synchronize the solar panel movement. The LST calculation subsystem is illustrated in Fig. 3 and developed using Equations (1) until (6) [16, 17].

$$\text{EoT} = 9.87 \sin(2\beta) - 7.53 \cos(\beta) - 1.5 \sin(\beta) \quad (1)$$

$$\beta = \frac{360}{365}\,(n - 81) \quad (2)$$

$$\text{TC} = 4\,(\text{longitude} - \text{LSTM} + \text{EoT}) \quad (3)$$

$$\text{TC} = 4\,(\text{LSTM} - \text{longitude}) + \text{EoT} \quad (4)$$

$$\text{LSTM} = 15^\circ . \Delta T_{\text{GMT}} \quad (5)$$

$$\text{LST} = \text{LT} + \frac{\text{TC}}{60} \quad (6)$$

The EoT, expressed in minutes in Eq. (1), represents the difference between solar time defined as time measured by the sun and standard clock time. This difference arises from Earth's elliptical orbit and axial tilt. The equation accounts for these variations, ensuring accurate timekeeping relative to the sun's position. In

Eq. (2), n represents the day of the year, where 1 corresponds to 1 January and 365 to 31 December. This factor converts the day of the year into an angular position along Earth's orbit, with 81 denoting the day on which the equation reaches its baseline value. The time correction (TC) accounts for the difference between a location's longitude and the standard time meridian (LSTM), combined with the Equation of Time (EoT).

The factor of 4 reflects Earth's rotation of 1° every 4 minutes. For locations east of the LSTM, TC is positive, advancing local solar time and resulting in earlier sunrise and solar noon, as shown in Eq. (3). For locations west of the LSTM, TC is negative, delaying local solar time and shifting sunrise and solar noon later, as shown in Eq. (4). In Eq. (5), ΔT_{GMT} represents the time difference from Greenwich Mean Time (GMT). For Malaysia, this corresponds to GMT +8, with LSTM = 120°. These adjustments ensure accurate local solar time, which is essential for precise solar tracking.

2.3. Hour angle (ω)

In Eq. (7), the hour angle (ω) represents the angular displacement of the sun from the local meridian, measured in degrees. The local meridian corresponds to solar noon, when the sun reaches its highest point in the sky. Due to the Earth's rotation of 15° per hour (or 1° every 4 minutes), a point on the Earth's surface experiences a daily cycle of day and night. The hour angle converts the time difference from solar noon into an angular displacement as:

$$\omega = 15° \text{ (LST - 12)} \tag{7}$$

Here, ω is expressed in degrees, and LST denotes the local solar time. When LST is later than 12:00, ω takes a positive value, indicating that the sun has moved west of the local meridian. On the other hand, when LST is earlier than 12:00, ω is negative, signifying that the sun is positioned east of the local meridian.

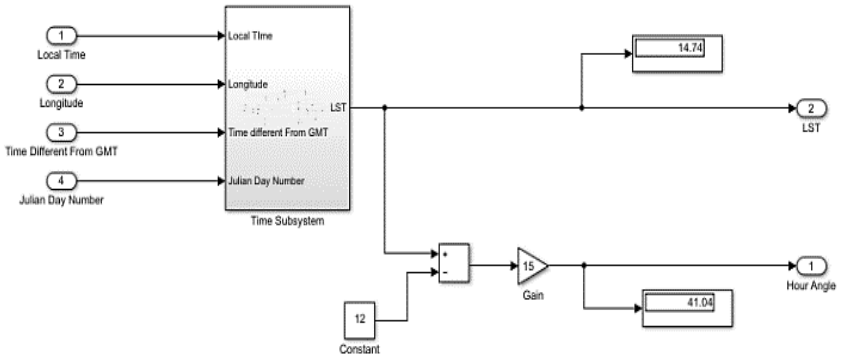

Fig. 3. MATLAB/Simulink model of the LST subsystem.

2.4. Declination angle (δ)

The declination angle (δ), as shown in Eq. (8), represents the tilt of the Earth's axis in relation to the sun. This angle fluctuates throughout the year due to the Earth's axial tilt and its orbit around the sun. It is crucial for determining the sun's altitude in the sky at any given time and location. The Earth's axial tilt is approximately

23.45°, leading to seasonal variations. The declination angle is equal to 0° only during the spring and fall equinoxes, as illustrated in Fig. 4.

$$\delta = 23.45 \sin\left[\frac{360}{365}(n-81)\right] \quad (8)$$

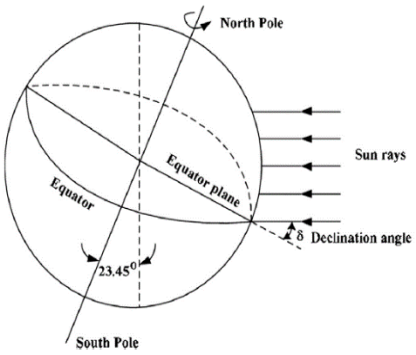

Fig 4. Declination angle [12].

2.5. Altitude angle (α) and Azimuth angle (σ)

The altitude and azimuth angles designed in the Simulink subsystem are illustrated in Fig. 5. The altitude angle (α), as indicated in Eq. (9), is the angle formed between the sun's incident rays and the observer's horizontal plane. It suggests the sun's angular height above the horizontal plane. This angle is crucial for adjusting the vertical tilt of the solar panel. It is influenced by the declination angle (δ), observer's latitude (φ), and hour angle (ω). Latitude (φ) is the geographic coordinate that specifies a point's north-south position on the Earth's surface.

$$\alpha = \sin^{-1}(\sin\delta \sin\varphi + \cos\delta \cos\varphi \cos\omega) \quad (9)$$

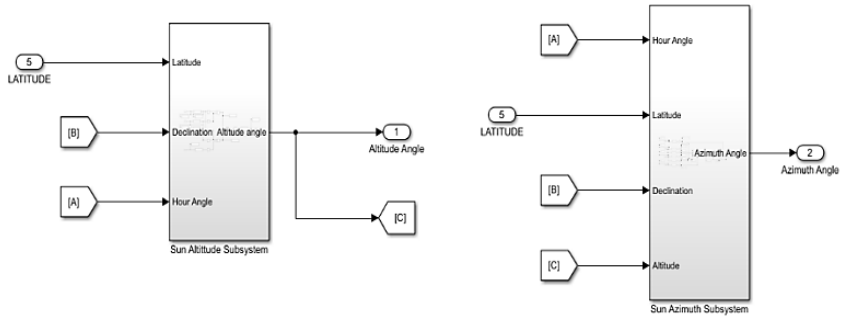

(a) Sun Altitude **(b) Sun Azimuth**

Fig. 5. Development of MATLAB/Simulink subsystem.

The azimuth angle (σ) indicates the compass direction of the sun relative to the true north. It is used to adjust the horizontal orientation of the solar panel, with values ranging from 0° (north) to 360° (clockwise) along the horizon. Eq. (10) takes into account the declination angle (δ), latitude (φ), hour angle (ω), and altitude angle (α) when LST is less than noon. If the LST exceeds noon, the calculation must be performed using Eq. (11).

$$\sigma = \cos^{-1}\left(\frac{\sin\delta\sin\varphi - \cos\delta\cos\varphi\cos\omega}{\cos\alpha}\right), \text{ for } LST < 12 \text{ or } \omega < 0 \quad (10)$$

$$\sigma = 360° - \cos^{-1}\left(\frac{\sin\delta\sin\varphi - \cos\delta\cos\varphi\cos\omega}{\cos\alpha}\right), \text{ for } LST > 12 \text{ or } \omega > 0 \quad (11)$$

$$\text{Tilt angle} = 180 - (90 + \alpha) \quad (12)$$

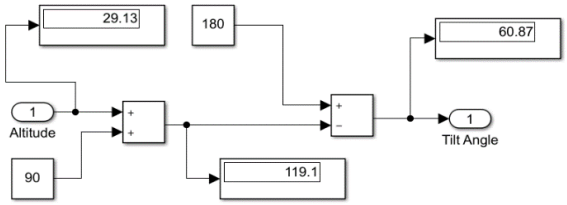

Fig. 6. Tilt angle calculation subsystem in MATLAB/Simulink.

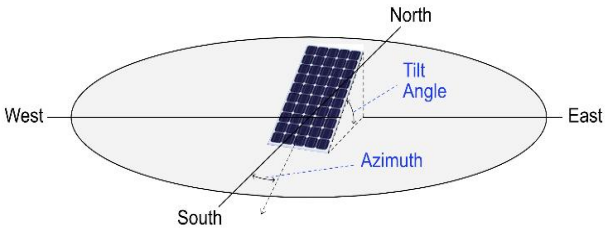

Fig 7. Illustration of tilt angle.

The tilt angle subsystem was based on the altitude values obtained, and Fig. 6 presents this subsystem, which was developed using Eq. (12). The tilt angle facing south for a location in the northern hemisphere, where the optimal fixed tilt angle is approximately equal to the latitude of the site as illustrates in Fig. 7. For example, at a latitude of 20°N, the best fixed tilt angle is about 20° facing south, ensuring that the panel surface is oriented to maximize solar energy absorption throughout the year.

3. Comparison of solar altitude, azimuth, and tilt angle

Solar data collected in Pagoh, Muar, Johor, Malaysia, a location near the equator are illustrated in Figs. 8 to 10. In particular, Fig. 8 shows the daily profiles of solar altitude, azimuth, and optimal tilt angle on 1 January. The altitude, represented by the black line, begins at 0° at sunrise, increases to a maximum of approximately 60-65° at solar noon, and then returns to 0° at sunset. This result indicates that even during the winter solstice period, Pagoh experiences relatively high solar altitudes due to its equatorial location.

The solar azimuth trajectory, shown by the red dashed line, starts at about 120° (southeast) at sunrise, shifts toward 180° (south) at noon, and ends around 240° (southwest) at sunset. This pattern reflects the shorter east-west solar path typically observed during this period. The tilt angle, illustrated by the blue line, demonstrates the continuous adjustments required for the solar panel to maintain an optimal perpendicular orientation to incoming solar radiation. The tilt angle increases from morning to noon and decreases toward sunset, confirming the

necessity of dual-axis tracking to maximize incident solar energy throughout the day. Comparison of the solar altitude and azimuth profiles for 1 January, 3 July, and 24 September is shown in Fig. 9.

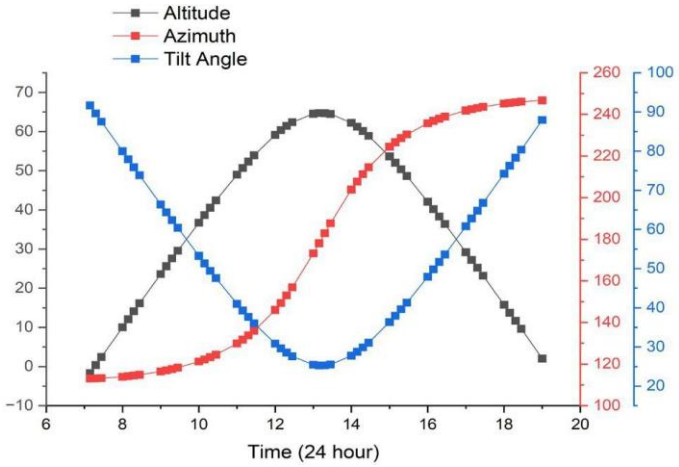

Fig. 8. Trend in altitude, azimuth, and tilt angle on 1 January.

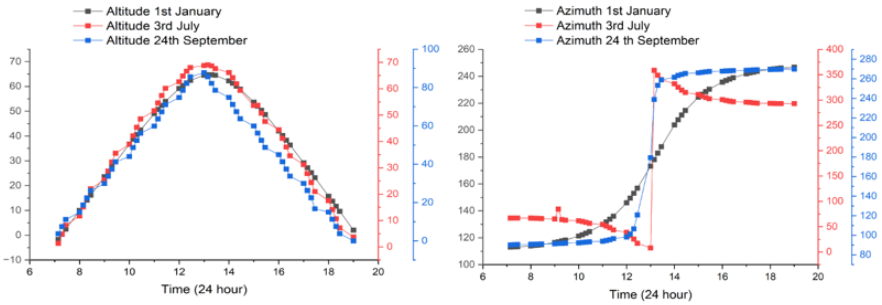

(a) Altitude angle. **(b) Azimuth angle.**

Fig. 9. Trend on 1 January, 3 July, and 24 September.

On 1 January, the maximum solar altitude reached approximately 60°, showing that even under weaker solar geometry the site still receives sufficient exposure for energy generation. By 3 July, the altitude rose to nearly 80°, resulting in intense and direct radiation that enhanced photovoltaic output and overall system performance. On 24 September, the peak altitude was around 70°, with day and night durations nearly equal. During this time, the Sun rises almost exactly in the east and sets almost exactly in the west, creating a balanced and symmetrical path. This transitional condition indicates stable solar availability and provides a useful reference point for evaluating tracking accuracy and seasonal system adjustments.

The 1 January profile occurred shortly after the winter solstice in the Northern Hemisphere, which typically falls around 21 or 22 December, when the Sun reaches its lowest annual elevation and the day length is shortest. In contrast, 3 July was close to the summer solstice, generally observed on 21 or 22 June, when the Sun reaches its highest position and the day length is longest. Meanwhile, 24

September was near the autumnal equinox, usually observed on 22 or 23 September, when day and night durations are nearly equal as the Sun crosses the equatorial plane. These astronomical events mark important transitions in Earth-Sun geometry and directly influence variations in solar altitude, azimuth displacement, and the optimal tilt angle throughout the year.

The azimuth angles exhibit distinct seasonal patterns where on 1 January, the Sun's path began at approximately 120° at sunrise in the southeast, shifted to 180° at noon facing south, and ended near 240° at sunset in the southwest. This trajectory produced a shorter horizontal range and reduced morning and evening exposure, which may limit energy capture for fixed or single-axis systems. On 3 July, the azimuth started near 60° at sunrise in the northeast, reached 180° at noon, and extended to about 300° at sunset in the northwest. The wider azimuth range reflected a longer daylight duration and a broader solar arc, thereby enhancing the potential for energy harvesting. On 24 September, the azimuth followed a symmetrical east-west trajectory, rising at 90° in the east, reaching 180° in the south at noon, and setting at 270° in the west. This pattern corresponded to nearly equal day and night durations, providing a stable reference for evaluating tracking performance and seasonal adjustments.

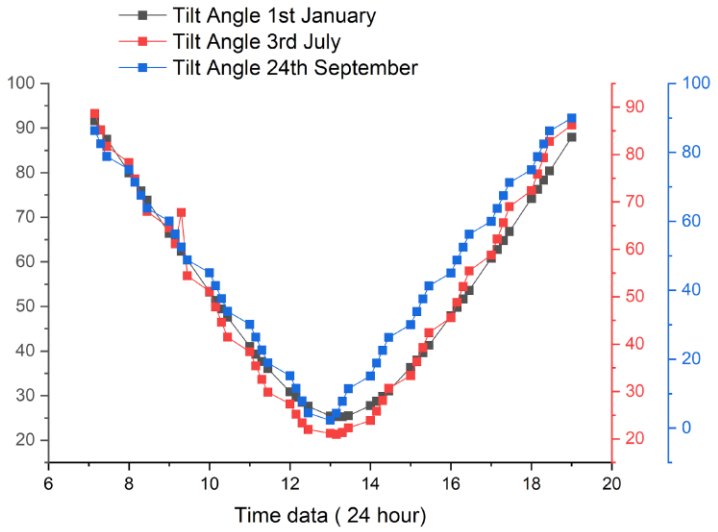

Fig. 10. Trend of tilt angle on 1 January, 3 July, and 24 September.

On 1 January, the tilt angle was lowest during the early morning and late afternoon, gradually rising toward midday before declining again in the evening, as shown in Fig. 10. This variation reflects the sun's lower altitude in the winter period, which requires larger panel adjustments to maintain optimal alignment with the solar rays. By 3 July, the tilt angle followed a broader adjustment range due to the sun's significantly higher altitude. The peak tilt appeared earlier in the day, and adjustments remained pronounced throughout the afternoon, allowing the system to capture maximum energy from the elevated summer trajectory. On 24 September, the tilt angle displayed an intermediate pattern between the winter and summer solstices.

With the sun passing more directly overhead, the adjustments were less extreme yet still necessary to sustain efficient energy capture across the day.

In conclusion, the variations in altitude, azimuth, and tilt angle observed throughout the year highlight their critical roles in maximizing solar energy efficiency. The substantial shifts in the Sun's position between solstices and equinoxes clearly show that a fixed solar panel cannot maintain optimal alignment, leading to significant reductions in energy yield. The results obtained demonstrate the necessity of a dynamic dual-axis tracking system capable of continuously adjusting both azimuth and tilt angles in response to real-time solar movement. Such adaptability ensures that the solar panel consistently achieves optimal orientation, thereby maximizing irradiance capture and improving overall system performance across all seasonal conditions in an equatorial environment.

4. Results and Discussion

The results of this study are presented in two main parts. First, the accuracy of the MATLAB/Simulink solar tracking model is examined through comparison with established web-based solar data tools. This comparison highlights the reliability of the simulation framework in predicting solar position and photovoltaic output under Malaysia's conditions. Second, the validated model is applied to experimental data collection, where the performance of tracking and non-tracking solar panel configurations is evaluated. The testing panel used is a 50 W monocrystalline module, with the current and voltage at maximum power under STC being 2.68 A and 18.68 V, respectively.

4.1. Data comparison between Gaisma and simulation model

The comparison of Gaisma solar data and SunEarthTool with the MATLAB simulation for Bandar Maharani, Muar (latitude 2.05° and longitude 102.56°) demonstrates strong agreement between the simulated results and real observations. These two sources were selected for validation because Gaisma provides widely used, location-specific solar data derived from long-term astronomical calculations, while SunEarthTool offers interactive, real-time solar position estimates based on global datasets. Hourly altitude data on 24 September were used as a benchmark due to the predictable solar geometry during the equinox. Across all sources, the altitude comparison shows a high degree of consistency, with the simulation aligning most closely with Gaisma. The differences between the simulation and Gaisma remain small, ranging from 0.00° to 0.98°, with an average deviation of 0.53°, confirming that the declination, hour angle, and altitude equations were correctly implemented.

SunEarthTool exhibits a slightly wider range of deviations, between 0.19° and 1.13°, along with one larger outlier of 13.167°, likely due to internal correction factors or time-conversion differences. Despite these variations, all datasets follow the same daytime altitude pattern, demonstrating consistent solar-position behaviour. The close agreement in Table 1 shows that the simulation model is reliable for calibration, performance checks, and further solar tracking analysis. Gaisma is helpful because it uses long-term astronomical data, making its results stable and dependable. SunEarthTool adds real-time solar calculations that adjust for time zones and location differences. Together, they provide both a solid reference and a practical check, making them effective tools for validating solar studies.

Table 1. Comparison of altitude and azimuth from MATLAB simulation, Gaisma and SunEarth tool.

Local time	Altitude from simula-tion	Altitude from Gaisma	Altitude from SunEarth Tool	Azimuth from simula-tion	Azimuth from Gaisma	Azimuth from SunEarth Tool
7.00	-15.02	-15	-15.26	89.53	89	89.98
8.00	-0.034	-0	-0.26	90.11	90	90.55
9.00	29.94	29	29.71	90.69	90	91.16
10.00	44.02	44	44.69	91.36	91	91.91
11.00	59.89	59	59.65	92.3	92	92.98
12.00	74.81	74	74.52	93.93	93	94.91
13.00	87.74	87	87.19	98.36	98	100.22
14.00	74.86	74	74.95	179.3	179	175.47
15.00	59.95	59	60.09	261.6	261	259.35
16.00	44.98	44	45.13	266.1	266	264.88
17.00	30	30	30.15	267.7	267	266.84
18.00	15.01	15	15.16	268.6	268	267.92
19.00	0.0254	0	0.17	269.3	269	269.24
20.00	-14.96	-14	-0.833	269.9	269	269.27

The azimuth comparison also indicates strong alignment among Gaisma, the simulation, and SunEarthTool. Deviations between the simulation and Gaisma range from approximately 0.11° to 1.30°, with most values below 1°, demonstrating accurate representation of the Sun's horizontal movement. SunEarthTool similarly follows the expected trend but with slightly larger deviations, between 0.22° and 2.16°, particularly around peak sun hours, likely due to differences in coordinate conventions or rounding methods. Importantly, all three datasets exhibit the same azimuth progression starting near the eastern horizon, shifting southward at solar noon, and moving toward the western horizon which further supporting the correctness of the simulation. The close agreement is significant because azimuth accuracy directly influences the orientation of dual-axis tracking systems, where even small angular errors can reduce irradiance capture and overall energy yield.

Overall, the strong agreement between the simulation and the two real-time tools confirms the reliability of the model and supports its application for analysing solar tracking behaviour and optimizing system orientation throughout the day. By closely following actual altitude and azimuth patterns, the simulation ensures precise tracking, maximizes irradiance capture, and improves the overall performance of solar energy systems under real-world conditions.

4.2. Performance comparison of tracking and non-tracking system

The performance of a dual-axis tracking PV system was compared against a fixed-tilt non-tracking system where the analysis considered maximum power (P_{max}), current at maximum power (I_{mp}) and voltage at maximum power (V_{mp}). The compiled data in Table 2 illustrates the hourly performance comparison between the tracking and non-tracking systems. During the early morning hours (8:00-9:00), the tracking system produced nearly three times the P_{max} of the fixed panel due to its superior alignment with the low-angle sunlight.

Throughout peak solar hour (12:00-16:00), the tracking system consistently maintained higher P_{max}, with gains of 12W-15W. This period reflects optimal

solar conditions, where dynamic tracking effectively minimizes angle-of-incidence losses. In the late afternoon (16:00-17:00), even as irradiance decreased, the tracking panels continued to outperform the fixed system, maintaining 5W-9W higher P_{max}. These results demonstrate that while the fixed-tilt system achieves peak efficiency only near solar noon, the tracking system continuously maximizes energy capture throughout the entire day.

The total energy captured by the tracking system was 690.1W, nearly double the 363.97W produced by the non-tracking system, resulting in an overall energy gain of 89.6%. The average maximum power output further demonstrates the advantage of tracking, with 18.65W for the tracking system compared to 9.84W for the fixed system. During the early morning and late afternoon as shown in Fig. 11, the increase in power was comparatively smaller, ranging from 2W to 5W, while no additional power was observed between 9:15 and 9:30, as the sun was already optimally aligned with the fixed panel. The tracking system consistently outperformed the fixed system in terms of current output. The I_{mp} in Fig. 12(a) ranged from 0.50-1.69A for the tracking system, compared to 0.25-1.16A for the non-tracking system. Peak gains in I_{mp} occurred during peak sun hour, reflecting the ability of the tracking system to maintain optimal panel orientation throughout the day.

For V_{mp}, both systems start at different voltage levels, with the tracking system showing a higher voltage from the beginning. Around 8:00 AM, the voltage difference is modest, but as the day progresses, the tracking system's voltage fluctuates less, maintaining relatively high values throughout the day. In contrast, the non-tracking system experienced fluctuations in V_{mp} due to its fixed orientation, particularly during early morning and late afternoon when the sun's altitude was low, as shown in Fig. 12(b). The superior performance of the dual-axis tracking system is directly attributed to its dynamic orientation, which maximizes the incident irradiance captured at each hour.

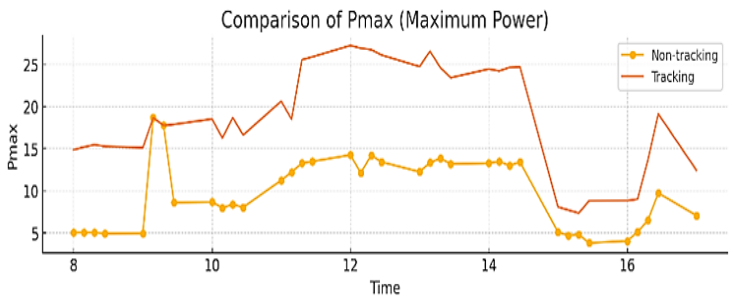

Fig. 11. Variation of power at maximum power.

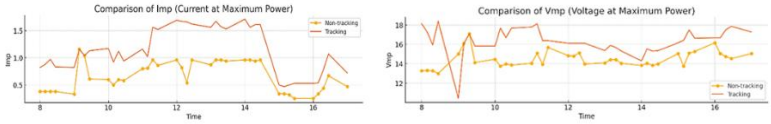

(a) Current. **(b) Voltage.**

Fig. 12. Variation of electrical parameters at maximum power.

Both P_{max} and I_{mp} measurements indicate higher current generation due to optimal sun alignment. The non-tracking system, constrained to a 10° south-facing tilt, was

unable to capture low and late-angle sunlight effectively, limiting overall energy production. In tropical regions like Pagoh, Johor, Malaysia, where solar angles change rapidly and cloud cover may vary, tracking systems provide significant advantages. The results highlight that a dual-axis tracking system not only nearly doubles energy capture compared to a fixed system but also maintains more consistent voltage and current outputs, optimizing overall PV system performance.

The superior performance of the dual-axis tracking system is directly attributed to its dynamic orientation, which maximizes the incident irradiance captured at each hour. Both P_{max} and I_{mp} measurements indicate higher current generation due to optimal sun alignment. Similarly, V_{mp} remained higher and more stable, reflecting improved voltage generation throughout the day. The non-tracking system, constrained to a 10° south-facing tilt, was unable to capture low and late-angle sunlight effectively, limiting overall energy production. In tropical regions like Pagoh, Johor, Malaysia, where solar angles change rapidly and cloud cover may vary, tracking systems provide significant advantages. The results highlight that a dual-axis tracking system not only nearly doubles energy capture compared to a fixed system but also maintains more consistent voltage and current outputs, optimizing overall PV system performance.

Table 2. Hourly performance comparison between the tracking and non-tracking systems.

Time	P_{max} Tracking (W)	P_{max} Non-Tracking (W)	Gain (W)	Time	P_{max} Tracking (W)	P_{max} Non-Tracking (W)	Gain (W)
8:00	14.86	5.04	9.82	12:45	26.11	13.42	12.69
8:15	15.20	5.05	10.15	13:00	24.74	12.25	12.49
8:30	15.46	5.04	10.42	13:15	26.55	13.34	13.21
8:45	15.28	4.93	10.35	13:30	24.61	13.84	10.77
9:00	15.10	4.95	10.15	13:45	23.42	13.20	10.22
9:15	18.66	18.66	0.00	14:00	24.45	13.27	11.18
9:30	17.76	17.76	0.00	14:15	24.22	13.48	10.74
9:45	17.88	8.61	9.27	14:30	24.64	13.00	11.64
10:00	18.52	8.67	9.85	14:45	24.71	13.42	11.29
10:15	16.26	7.98	8.28	15:00	8.08	5.11	2.97
10:30	18.68	8.38	10.30	15:15	7.71	4.67	3.04
10:45	16.61	8.04	8.57	15:30	7.35	4.82	2.53
11:00	20.63	11.24	9.39	15:45	8.81	3.81	5.00
11:15	18.49	12.22	6.27	16:00	8.84	4.04	4.80
11:30	25.55	13.27	12.28	16:15	9.00	5.11	3.89
11:45	25.89	13.48	12.41	16:30	13.65	6.49	7.16
12:00	27.24	14.25	12.99	16:45	19.12	9.73	9.39
12:15	26.92	12.12	14.80	17:00	12.44	7.07	5.37
12:30	26.75	14.21	12.54				

5. Conclusions

This study presents a simulation-based dual-axis solar tracking model tailored to Malaysia's equatorial climate. The model uniquely integrates precise conversion of

local clock time to LST with dynamic calculation of solar altitude, azimuth, and tilt angles, enabling continuous and accurate panel orientation. Validation against Gaisma solar data and the SunEarthTool website confirmed the model's accuracy, demonstrating both reliability and practical relevance for tropical environments. The analysis addresses a critical research gap by evaluating dual-axis tracking performance in equatorial regions, where seasonal variation is limited but daily changes in solar angles remain significant, requiring continuous tilt and azimuth adjustments.

Performance comparisons show that the tracking system consistently outperforms fixed-tilt panels across all key parameters (P_{max}, I_{mp}, and V_{mp}). Early morning P_{max} was nearly three times higher than the non-tracking system, while stable I_{mp} and V_{mp} during peak sunlight hours highlight the effectiveness of dynamic sun alignment. These findings establish the dual-axis tracking system as a substantial advancement for solar energy harvesting in tropical climates, where variable irradiance and shifting sun angles challenge fixed-panel systems.

The novelty of this work lies in providing a localized, simulation-based framework validated against real-world solar data, bridging the gap between theoretical MATLAB models and practical application. This contribution demonstrates the tangible benefits of adaptive tracking for Malaysia's renewable energy goals.

While limited to simulation-based analysis, future studies should extend the framework with sensor feedback, predictive weather modelling, and long-term field testing to further enhance system performance.

Acknowledgement

This research was supported by Universiti Tun Hussein Onn Malaysia (UTHM) through Tier 1 (vot Q881).

Nomenclatures

n	Day of the year

Greek Symbols

σ	Azimuth angle.
Θ	Angle of incidence
δ	Declination.
ω	Hour angle
φ	Latitude.

Abbreviations

EoT	Equation of Time
GMT	Greenwich Mean Time
LST	Local solar time
LSTM	Standard time meridian
PV	Photovoltaic
TC	Time correction

References

1. Yeung, C.; Wang, J.; Du, Y.; Cao, J.; Ding, Y.; Chen, M.; Zhao, W.; and Jia, C. (2024). Research on solar irradiance distribution and correlation with photovoltaic generated output: A case study of Wuhan and Zhangbei, China. *Proceedings of the 2024 IEEE/IAS 60th Industrial and Commercial Power Systems Technical Conference*, (*I&CPS*), Las Vegas, NV, USA, 1-6.
2. Elavarasan, R.M.; Nadarajah, M.; and Shafiullah, G.M. (2024). Multi-criteria decision analysis of clean energy technologies for envisioning sustainable development goal 7 in Australia: Is solar energy a game-changer? *Energy Conversion and Management*, 321, 119007.
3. Koerner, S.A.; Siew, W.S.; Salema, A.A.; Balan, P.; Mekhilef, S.; and Thavamoney, N. (2022). Energy policies shaping the solar photovoltaics business models in Malaysia with some insights on Covid-19 pandemic effect. *Energy Policy*, 164, 112918.
4. Muhammad-Sukki, F.; Abu-Bakar, S.H.; Munir, A.B.; Yasin, S.H.M.; Ramirez-Iniguez, R.; McMeekin, S.G.; Stewart, B.G.; and Rahim, R.A. (2014). Progress of feed-in tariff in Malaysia: A year after. *Energy Policy*, 67, 618-625.
5. Sustainable Energy Development Authority (SEDA). (2021). Retrieved October 5, 2020, from www.seda.gov.my
6. Singh, A.K.; and Singh, R.R. (2021). An overview of factors influencing solar power efficiency and strategies for enhancing. *Proceedings of the 3rd IEEE International Virtual Conference on Innovations in Power and Advanced Computing Technologies* (*i-PACT*), Kuala Lumpur, Malaysia, 1-6
7. Taha, M.T.; Mohamed, E.O.; Abdolsalam, A.M.; and Taha, A.B. (2021). Control of single-axis and dual-axis solar tracking system. *Proceedings of the 2020 International Conference on Computer*, *Control*, *Electrical*, *and Electronics Engineering*, (*ICCCEEE*), Khartoum, Sudan, 1-6.
8. Mamodiya, U.; and Tiwari, N. (2021). Design and implementation of an intelligent single axis automatic solar tracking system. *Materials Today: Proceedings*, 81(2), 1148-1151.
9. Reza, M.N.; Hossain, M.S.; Mondol, N.; and Kabir, M.A. (2021). Design and implementation of an automatic single axis solar tracking system to enhance the performance of a solar photovoltaic panel. *Proceedings of the 2021 International Conference on Science and Contemporary Technologies* (*ICSCT*), Dhaka, Bangladesh,1-6.
10. Zhu, Y.; Liu, J.; and Yang, X. (2020). Design and performance analysis of a solar racking system with a novel single-axis tracking structure to maximize energy collection. *Applied Energy*, 264, 114647.
11. Awasthi, A.; Shukla, A.K.; Murali Manohar S.R.; Dondariya, C.; Shukla, K.N.; Porwal, D.; and Richhariya, G. (2020). Review on sun tracking technology in solar PV system. *Energy Reports*, 6, 392-405.
12. Cheng, E.M.; Tan, R.H.; and Loong, K.W. (2022). Performance evaluation of tracking limit on single axis tracking photovoltaic system in Malaysia. *Proceedings of the 2022 International Conference on Green Energy*, *Computing and Sustainable Technology* (*GECOST*), Miri Sarawak, Malaysia, 18-23.

13. Sharma, N.; Puri, V.; and Kumar, G. (2021). Relative design and investigation of fixed/single axis and dual axis tracking system for diverse weather conditions. *Proceedings of the 2021 5th International Conference on Electrical, Electronics, Communication, Computer Technologies and Optimization Techniques (ICEECCOT)*, Mysuru, India, 118-124.
14. Sowaruth, N.; and Ramful, R. (2023). Analysis of a dual-axis 20W-rated photovoltaic solar tracker. *Applied Solar Energy*, 59(6), 865-877.
15. Ishak, M.H.B.; Burham, N.; Masrie, M.; Janin, Z.; and Sam, R. (2023). Automatic dual-axis solar tracking system for enhancing the performance of a solar photovoltaic panel. *Proceedings of the 2023 - 9th IEEE International Conference on Smart Instrumentation, Measurement and Applications*, (*ICSIMA*), Kuala Lumpur, Malaysia, 279-283.
16. Arisotya, Y.B.; Primawan, A.B.; and Suwarno, D.U. (2022). Dual axis solar tracker with fuzzy logic method. *Proceedings of the 2022 International Conference on Informatics Electrical and Electronics* (*ICIEE*), Yogyakarta, Indonesia, 1-5.
17. Jazayeri, K.; Uysal, S.; and Jazayeri, M. (2013). MATLAB/simulink based simulation of solar incidence angle and the sun's position in the sky with respect to observation points on the Earth. *Proceedings of the 2013 International Conference on Renewable Energy Research and Applications*, (*ICRERA*), Madrid, Spain, 173-177.
18. Jha, S.K.; Roy, S.; Singh, V.K.; and Mishra, D.P. (2020). Sun's position tracking by solar angles using MATLAB. *Proceedings of the International Conference on Renewable Energy Integration into Smart Grids: A Multidisciplinary Approach to Technology Modelling and Simulation* (*ICREISG*), Bhubaneswar, India, 5-9.